Synthetic Metals 199 (2015) 280–283

Contents lists available at ScienceDirect

Synthetic Metals

journal homepage: www.elsevier.com/locate/synmet

Short communication

Novel conjugated polymer for organic photovoltaics: Synthesis and device optimization

Bong-Gi Kim [a,*], Hui Joon Park [b,**]

[a] Dongjin Semichem Co., Ltd., 613, Sampyung-Dong, Bundang-Gu, Seongnam-Si, Gyeonggi-Do 463-400, South Korea
[b] Division of Energy Systems Research, Ajou University, Suwon 443-749, South Korea

ARTICLE INFO

Article history:
Received 30 November 2014
Accepted 4 December 2014
Available online 9 December 2014

Keywords:
Conjugated polymer
Organic photovoltaics
Intramolecular charge transfer
Aggregation

ABSTRACT

A novel conjugated polymer, TdTB, having an alternating configuration of electron donor and acceptor was synthesized for organic photovoltaic (OPV) application. Intramolecular charge transfer made TdTB exhibit bimodal-shaped absorption in visible region, which secured about 4% power conversion efficiency (PCE) via enhanced absorption efficiency. OPV cells could be further optimized by means of additive-assisted annealing or additional super critical CO_2 liquid treatment after additive annealing, and more developed TdTB aggregation was achieved. Consequently, their performances were dramatically improved about 17% and 33%, compared to the non-annealed PV cell, giving 4.65 and 5.27% PCEs, respectively.

1. Introduction

Organic photovoltaic (OPV) cells adopting conjugated polymers (CPs) have drawn great attention as a cost-effective alternative to silicon-based solar cells. The power conversion efficiency (PCE) of OPV cell has been rapidly enhanced during the last couple of years and currently exceeds 6% [1–6]. This dramatic improvement of OPV performance could be ascribed to the development of new materials, mostly CPs, and to the growing understanding of OPV operation principles [1–11]. One of the fundamental requirements for photovoltaic energy conversion is the collection of photon as much as possible. In this regard, there have been lots of efforts to match the absorption range of CP to the high photon flux region of the solar spectrum, including the energy level modulation of CP by means of computational calculations. The most promising strategy for tailoring the CP band-gap involves introducing donor (D) and acceptor (A) monomers together into the polymer framework [12,13]. The underlying concept is that the interaction between alternating electron-rich donors and electron deficient acceptors results in a compressed band-gap via molecular orbital hybridization and intra-molecular charge transfer.

Moreover, it is also well known that the film morphology, mostly induced by the aggregation of CP, decisively determines OPV performance, because the aggregation facilitates intermolecular charge transfer via strong π–π interaction, which results in outperforming electrical mobility. To enhance the crystallinity of CP, several film-forming techniques have been reported, such as thermal treatment [14], additive-assisted annealing [15], and super-critical liquid treatment [16].

In order to address these points, in this contribution, we designed and synthesized a novel low band-gap CP that could secure considerable absorption efficiency. Furthermore, the performances of OPV cells, prepared by several film fabrication techniques, were characterized to verify the effects of those fabrication process on the performances.

2. Experimental

2.1. Compound 2

Under Ar condition, compound 1 (1 g, 5.43 mmol) and NaH (0.65 g, 3.0 eq) were stirred in anhydrous DMF at 60 °C for 30 min. After adding 2-ethylhexyl bromide (3.86 ml, 21.7 mmol) slowly at room temperature, the mixture was stirred for 24 h at 60 °C. Then, water was added to quench the mixture, and the mixture was extracted with diethyl ether. The extracted organic solution was dried with $MgSO_4$, and solvent was evaporated *in vacuo*. Compound 2 (73%) was obtained from column chromatography using an eluent of dichloromethane. Compound 1, 2, 3 and 4 are denoted in Scheme 1. ^{1}H-NMR (400 MHz, CDCl3) δ 6.73 (s, 2H), 3.38 (s, 4H), 2.28 (d, 4H), 2.71 (s, 4H), 1.49 (m, 2H), 1.2–1.35 (m, 16H), 0.8–0.9 (m, 12H), and *m/z* EIMS 409.

* Corresponding author. Tel.: +82 31 627 3536.
** Corresponding author. Tel.: +82 31 219 2577.
E-mail addresses: bgkim@dongjin.com (B.-G. Kim), huijoon@ajou.ac.kr (H.J. Park).

http://dx.doi.org/10.1016/j.synthmet.2014.12.010
0379-6779/

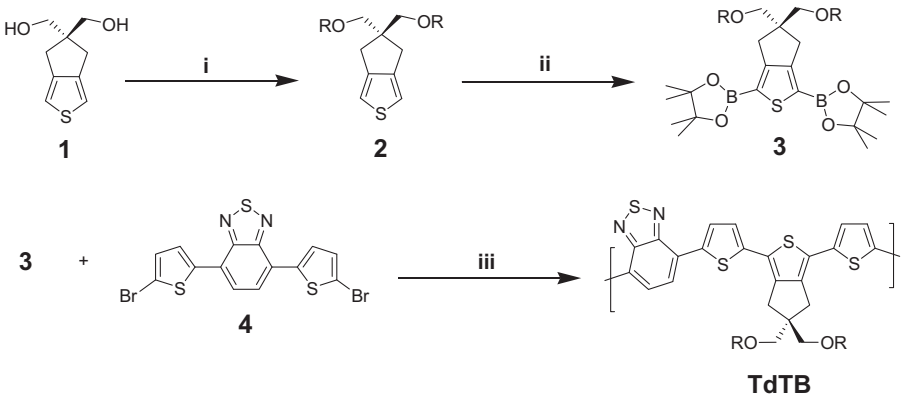

Scheme 1. Synthetic procedures of TdTB. R indicates 2-ethylhexyl group. (i) 2-Ethylhexyl bromide, NaH, DMF, 60 °C, 24 h, (ii) bis(pinacolato) diboron, DBP, Ir(I), heptanes/hexane, 50 °C, 16 h, (iii) Pd(0), tetraethyl ammonium hydroxide, water, 90 °C, 36 h.

2.2. Compound 3

Under Ar condition, compound 2 (1 g, 2.45 mmol), 4.4′-di-tert-butyl-2.2′-bipyridine (DBP) (19.845 mg, 3.0 mol%) and bis(pinacolato) diboron (0.497 g, 1.96 mmol) were added to heptanes. After adding bis(1,5-cyclooctadiene) di-μ-methoxydiiridium(I) (Ir(I)) (24.01 mg, 0.04 mmol), the mixture was stirred at 50 °C for 16 h and poured into cold water. Then, the mixture was extracted with chloroform and dried with $MgSO_4$. Compound 3 (65%) was obtained from column chromatography after elution of chloroform/hexane (1:5). ^{1}H-NMR (400 MHz, CDCl3) δ 3.40 (s, 4H), 2.28 (d, 4H), 2.71 (s, 4H), 1.49 (m, 2H), 1.2–1.35 (m, 40H), 0.8–0.9 (m, 12H), and *m*/*z* EIMS 661.

2.3. TdTB

Under inert conditions (Ar), compound 3 was dissolved into toluene, and the equivalent amount of corresponding monomer (compound 4) was mixed. After adding 5 mol% of tetrakis (triphenylphosphine) palladium(0) (Pd(0)) and 1.8 ml of tetraethyl ammonium hydroxide (20% solution), the mixture was stirred at 90 °C for 36 h. Bromobenzene (24 μm) and benzene boronic acid (26 mg) were added respectively to the mixture for chain end modification. The final polymer was collected via reprecipitation into methanol. The solid was collected through 0.45 μm nylon filter and washed with methanol and acetone in a soxhlet apparatus to remove the oligomers and catalyst residue. After dissolving obtained polymer into chloroform, the polymer solution was eluted through a column, packed with Cellite and Florosil. Then, the solution was concentrated and reprecipitated from methanol again (Mn:21500, Mw: 35470, and PDI: 1.65).

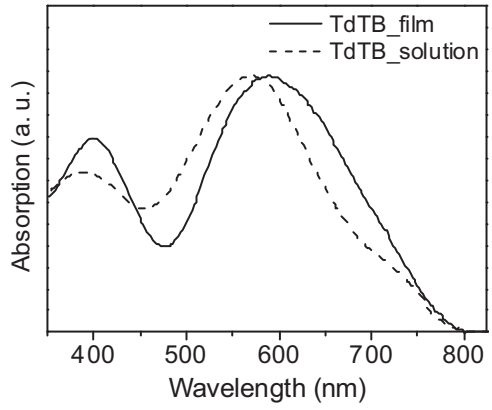

Fig. 1. UV–vis absorption of obtained TdTB both in solution (chloroform) and film.

2.4. Film preparation for OPV device

PCBM[70] was purchased from SES research and used without further purification. After dissolving obtained TdTB (10 mg) and PCBM[70] (15 mg) into *o*-dichlorobenzene (1.0 mL), the mixture was filtered with a syringe filter (0.45 μm pore diameter) and used to form an active layer by means of spin-casting. In case of additive-assisted annealing, 1,8-octanedithiol (8.0 μL) was added to the TdTB:PCBM[70] blend solution, and the same procedure was utilized to obtain an active layer. To additionally treat the active layer with super critical CO_2 liquid, the film that contains the additive was left into the closed chamber filled with CO_2 gas under 1500 psi at 35 °C for 30 min.

2.5. OPV device fabrication

ITO-coated glass was cleaned with acetone and IPA followed by UV ozone treatment for 10 min. PEDOT:PSS (Baytron PH 1000) was spin-cast on the substrate and baked at 140 °C for 15 min. TdTB:PCBM[70] blend solution was spin-cast at 700 rpm for 30 s and the blend film was used for metal electrode evaporation without further treatment. Final devices were fabricated by depositing 1 nm-thick LiF and 70 nm Al layer (9.6 mm^2) sequentially under 5×10^{-7} Torr (1 Torr = 133.32 Pa). All devices were characterized under nitrogen and the typical illumination intensity was 100 mW/cm^2 (AM 1.5G Oriel solar simulator).

3. Results and discussion

As illustrated in Scheme 1, terthiophene and 2,1,3-benzothiadiazole were adopted as electron donating and accepting moieties, respectively for D-A type alternating configuration. All starting materials were purchased from the commercial suppliers (Aldrich and Fisher Sci.), and the detailed synthetic procedures are summarized in Section 2. Monomers, compound 3 and compound 4, were prepared as previously described [17,18], and their

Table 1
Summary of OPV device performance obtained with TdTB and additional processes.

Process	None	Additive	Additive + CO_2
V_{oc} (V)	0.88	0.85	0.8
J_{sc} (mA)	9.95	10.93	12.29
FF (%)	45.4	50	53.7
PCE (%)	3.97	4.65	5.27

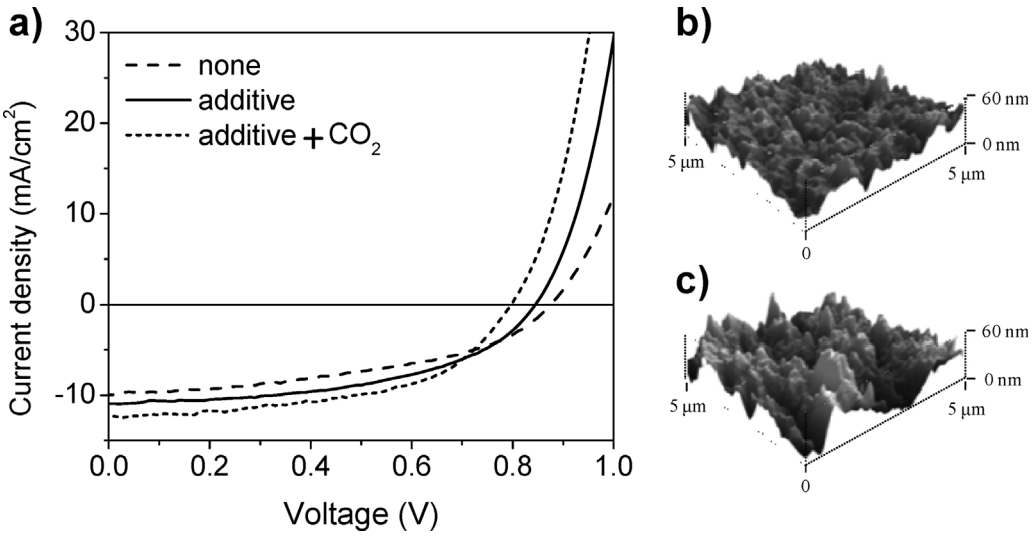

Fig. 2. (a) *J–V* curves of OPV devices adopting TdTB and PCBM[70]. (b) and (c) indicate surface morphology of films prepared with additive-assisted annealing only and both additive-assisted annealing and further CO_2 liquid-assisted annealing, respectively.

chemical structures were fully characterized with ^{1}H-NMR and GC-mass. Final CP (TdTB) was obtained through Suzuki-type polymerization under Pd(0) catalysis. As shown in Fig. 1, TdTB exhibited bimodal-shaped absorption, a characteristic absorption phenomenon in D-A type CPs, both in solution and film. In general, the absorption in shorter wavelength is originated from the molecular orbital hybridization of repeating unit without intra-molecular charge transfer. Here, the intra-molecular charge transfer in D-A type chain configuration makes CP chain planar, finally producing another absorption band in longer wavelength region. The absorption intensity both in shorter and longer wavelength region can be tuned by manipulating intrinsic chain planarity of CPs. The absorption intensity in shorter wavelength relatively decreases compared to that in longer wavelength as the chain planarity of CP increases. This implies that obtained TdTB has decent chain planarity, which would be helpful to induce π–π interaction for inter-chain aggregation in solid film. Indeed, TdTB exhibited absorption red-shift in film, a direct evidence of CP aggregation.

We fabricated OPV device after blending TdTB with PCBM[70], and the device performances were characterized depending on the film preparation processes. Thermally annealed devices produced poorer performance because of strong recombination as similarly demonstrated in our previous work [19]. Thus, the device adopting TdTB was optimized without any treatment, and the best performance was achieved utilizing 1:1.5 blending ratio of TdTB:PCBM[70]. Then, the device was further optimized, by means of additive-assisted annealing and super critical CO_2 liquid treatment, to additionally improve TdTB aggregation. In case of additive-assisted annealing, 1,8-octandithiol (8 vol%) was mixed with TdTB:PCBM[70] blend solution having 1:1.5 blending ratio, and the active layer was prepared through spin-casting without any thermal treatment. As for the super critical CO_2 liquid-treated film, additive-assisted film was additionally exposed to the closed chamber, filled with CO_2 gas at 35 °C for 30 min under 1500 psi. When OPV performances were compared (Table 1 and Fig. 2a), PV cells with additive- or CO_2- treated active layer exhibited slightly reduced open-circuit voltage (V_{oc}), compared to the none-treated device, but overall PCEs were dramatically improved about 17% and 33%, respectively, mainly due to the improvement of short-circuit current (J_{sc}) and fill factor (FF). The V_{oc} drop could be ascribed to the enhanced aggregation, induced by additive or CO_2 liquid, because the aggregation of CP augments charge recombination around the interface between CP and PCBM[70], ultimately decreasing V_{oc} [19]. However, the enhanced aggregation provides better phase separation between CP and PCBM[70] for higher fill factor as well as carrier mobility, leading to improved current density in OPV device. To verify the process-assisted aggregation, we investigated film morphologies with atomic force microscopy (AFM) because the surface roughness is one of crucial evidences that can explain the degree of aggregation of CP. The film obtained without any treatments had no noticeable feature with 1.84 nm of room-mean-square (RMS) roughness. However, the film roughness turned out to be increased when additive was incorporated (Fig. 2b, RMS; 6.74 nm), and it was further augmented after CO_2 liquid treatment (RMS; 11.43). This implies that those additional processes, additive- and CO_2 liquid-assisted annealings, were effective to improve TdTB aggregation, which resulted in higher current density including better fill factor in OPV devices.

4. Conclusion

A novel CP, TdTB, was synthesized for OPV application. TdTB exhibited bimodal-shaped absorption because of intra-molecular charge transfer, and its absorption was slightly red-shifted when casted to thin film format. Judging from the absorption intensity in longer wavelength region, it is confirmed that TdTB has decent chain planarity, which facilitates inter-chain interaction for aggregation. OPV device, fabricated by TdTB:PCBM[70] blend (1:1.5 blending ratio), showed about 4% PCE without any film annealing. To additionally improve OPV device performances, we applied additive-assisted annealing or additional CO_2 liquid-assisted annealing after additive treatment, and their PCEs were dramatically enhanced about 17% and 33%, respectively, because those processes effectively improved TdTB aggregation. The film morphologies, characterized by means of AFM, confirmed that the additive- and CO_2 liquid-assisted annealing were helpful to induce TdTB aggregation.

References

[1] H.-Y. Chen, J. Hou, S. Zhang, Y. Liang, G. Yang, Y. Yang, L. Yu, Y. Wu, G. Li, Nat. Photonics 3 (2009) 649.
[2] H. Zhou, L. Yang, A.C. Stuart, S.C. Price, S. Liu, W. You, Angew. Chem. Int. Ed. 50 (2011) 2995–2998.
[3] Y. Zhang, J. Zou, H.-L. Yip, K.-S. Chen, D.F. Zeigler, Y. Sun, A.K.-Y. Jen, Chem. Mater. 23 (2011) 2289–2291.
[4] C. Piliego, T.W. Holcombe, J.D. Douglas, C.H. Woo, P.M. Beaujuge, J.M.J. Fréchet, J. Am. Chem. Soc. 132 (2010) 7595–7597.

[5] S.H. Park, A.S. Roy Beaupré, S. Cho, N. Coates, J.S. Moon, D. Moses, M. Leclerc, K. Lee, A.J. Heeger, Nat. Photonics 3 (2009) 297.
[6] Y. Liang, Z. Xu, J. Xia, S.-T. Tsai, Y. Wu, G. Li, C. Ray, L. Yu, Adv. Mater. 22 (2010) E135–E138.
[7] A. Tada, Y. Geng, Q. Wei, K. Hashimoto, K. Tajima, Nat. Mater. 10 (2011) 450.
[8] S.K. Pal, T. Kesti, M. Maiti, F. Zhang, O. Inganäs, S. Hellström, M.R. Andersson, F. Oswald, F. Langa, T.Ö. sterman, T. Pascher, A. Yartsev, V. Sundström, J. Am. Chem. Soc. 132 (2010) 12440–12451.
[9] J.-L. Brédas, J.E. Norton, J. Cornil, V. Coropceanu, Acc. Chem. Res. 11 (2009) 1691.
[10] D.H. Wang, D.Y. Kim, K.W. Choi, J.H. Seo, S.H. Im, J.H. Park, O.O. Park, A.J. Heeger, Angew. Chem. Int. Ed. 50 (2011) 5519–5523.
[11] J.K. Lee, W.L. Ma, C.J. Brabec, J. Yuen, J.S. Moon, J.Y. Kim, K. Lee, G.C. Bazan, A.J. Heeger, J. Am. Chem. Soc. 130 (2008) 3619–3623.
[12] J. Peet, J.Y. Kim, N.E. Coates, W.L. Ma, D. Moses, A.J. Heeger, G.C. Bazan, Nat. Mater. 6 (2007) 497.
[13] N. Blouin, A. Michaud, M. Leclerc, Adv. Mater. 19 (2007) 2295–2300.
[14] S. Cho, K. Lee, J. Yuen, G. Wang, D. Moses, A.J. Heeger, M. Surin, R. Lazzaroni, J. Appl. Phys. 100 (2006) 114503.
[15] J.-F. Chang, B. Sun, D.W. Breiby, M.M. Nielsen, T.I. Solling, M. Giles, I.M. Culloch, H. Sirringhaus, Chem. Mater. 16 (2004) 4772.
[16] J. Amonoo, E. Glynos, X.C. Chen, P.F. Green, J. Phys. Chem. 116 (2012) 20708.
[17] B.-G. Kim, E.J. Jeong, J.W. Chung, S. Seo, B. Koo, J. Kim, Nat. Mater. 12 (2013) 659.
[18] Y.-J. Cheng, J.-S. Wu, P.-I. Shih, C.-Y. Chang, P.-C. Jwo, W.-S. Kao, C.-S. Hsu, Chem. Mater. 23 (2011) 2361.
[19] B.-G. Kim, E.J. Jeong, H.J. Park, D. Bilby, L.J. Guo, J. Kim, ACS Appl. Mater. Interfaces 3 (2011) 674.